



Validity of the LTD-DHT Shaw and Thellier palaeointensity methods: a case study of the Kilauea 1970 lava

Yusuke Oishi^{a,1}, Hideo Tsunakawa^{a,*}, Nobutatsu Mochizuki^a, Yuhji Yamamoto^b,
Ken-Ichi Wakabayashi^a, Hidetoshi Shibuya^c

^a Department of Earth and Planetary Sciences, Tokyo Institute of Technology, Tokyo 152-8551, Japan

^b Geological Survey of Japan, AIST, Tsukuba, Ibaraki 305-8567, Japan

^c Department of Earth Science, Kumamoto University, Kumamoto 860-8555, Japan

Received 20 April 2004; received in revised form 4 October 2004; accepted 11 October 2004

Abstract

The double heating technique of the Shaw method with low-temperature demagnetisation (LTD-DHT Shaw method) for determination of geomagnetic palaeointensity is applied to samples exhibiting high-temperature oxidation states from the Kilauea 1970 lava, Hawaii Island. Results are obtained for 11 of the 12 specimens prepared from five block samples, yielding an average palaeointensity of $38.2 \pm 2.8 \mu\text{T}$ ($N = 11$, $\pm 1\sigma$). This value is consistent with the expected value determined from DGRF 1970 ($35.8 \mu\text{T}$), and does not appear to be significantly dependent on the high-temperature oxidation state. Coe's version of the Thellier method was also applied to nine specimens prepared from the same block samples, and successful results were obtained for seven specimens, giving an average palaeointensity of $43.2 \pm 8.4 \mu\text{T}$ ($N = 7$). Although this average is statistically consistent with the expected value, the results include erroneously high palaeointensities (52.1 and $55.4 \mu\text{T}$) for specimens from one block sample of intermediate high-temperature oxidation state. The present results therefore reinforce the broader applicability of the LTD-DHT Shaw method for samples with high-temperature oxidation states compared with Coe's version of the Thellier method. It is also shown that the samples yielding overestimated Thellier palaeointensities tend to fall close to the mixing line between single-domain (and/or pseudo-single-domain) and multidomain components on the Day plot. This relationship may be useful as a pre-selection technique for application of the Thellier method.

© 2004 Elsevier B.V. All rights reserved.

Keywords: Palaeointensity; Shaw method; Thellier method; Kilauea lava; High-temperature oxidation; Day plot

1. Introduction

Correct determination of the absolute intensity of the ancient geomagnetic field is important for investigating the evolution of the geodynamo and the related conditions in the earth's deep interior. The Thellier

* Corresponding author. Tel.: +81 3 5734 2459;
fax: +81 3 5734 3537.

E-mail address: htsuna@geo.titech.ac.jp (H. Tsunakawa).

¹ Present address: Department of Earth and Planetary Science,
University of Tokyo, Tokyo 113-0033, Japan.

method (Thellier and Thellier, 1959) applied to natural remanent magnetisation (NRM) of thermoremanent magnetisation (TRM) origin is considered at present to be the most reliable means of determining the geomagnetic palaeointensity. Since thermal alteration of the sample during heating in the Thellier experiments can impair the results, the partial thermoremanent magnetisation (pTRM) check (Coe, 1967) is generally employed to detect thermal alteration due to laboratory heating. Nevertheless, several studies using natural and artificial samples have indicated that the Thellier method often gives an incorrect palaeointensity (e.g. Tanaka and Kono, 1991; Kosterov and Prévot, 1998; Calvo et al., 2002; Yamamoto et al., 2003; Biggin and Thomas, 2003; Mochizuki et al., 2004), and many improvements to the Thellier method have been proposed (e.g. Valet, 2003). It should also be noted that the database of Thellier palaeointensities possibly includes a positive bias, as almost all incorrect values reported to date have been overestimates.

The Shaw method (Shaw, 1974) is an alternative method for determining the palaeointensity in which samples are heated above the Curie temperatures in the laboratory to give a full TRM. The method has since been modified to incorporate a correction technique for thermal alteration of the samples due to laboratory heating (e.g. Kono, 1978; Tsunakawa and Shaw, 1994). Yamamoto et al. (2003) and Mochizuki et al. (2004) applied the double heating technique of the Shaw method with low-temperature demagnetisation (LTD-DHT Shaw method; Tsunakawa et al., 1997; Yamamoto et al., 2003) to samples from the Kilauea 1960 lava and the Oshima 1986 lava, respectively. The LTD-DHT Shaw method is an improved version of the Shaw method, utilising anhysteretic remanent magnetisation (ARM) correction, the double heating technique, and LTD treatment. In the original Shaw method, sample alteration due to laboratory heating was checked based on the agreement between ARM coercivity spectra obtained before and after laboratory heating (Shaw, 1974). The ARM correction technique (e.g. Kono, 1978; Rolph and Shaw, 1985) allows for the correction of laboratory-induced TRM due to sample alteration during laboratory heating. This technique assumes that the ARM coercivity spectra are analogous to the TRM. In the single heating version of the modified Shaw method, this assumption is examined mainly by the linearity of the diagram of NRM versus TRM

after ARM correction (e.g. Rolph and Shaw, 1985). In the double heating technique, the sample is heated twice in the same laboratory field, and the applicability of the ARM correction is also examined by agreement between the first and second TRM after ARM correction (Tsunakawa and Shaw, 1994). The LTD treatment prevents possible effects due to multidomain (MD) components (Tsunakawa et al., 1997; Yamamoto et al., 2003).

The LTD-DHT Shaw method has been applied to a few lavas with high-temperature oxidation states, yielding average palaeointensities of $35.7 \pm 3.3 \mu\text{T}$ ($N=7$) for the Kilauea 1960 lava (Yamamoto et al., 2003) and $46.4 \pm 4.7 \mu\text{T}$ ($N=6$) for the Oshima 1986 lava (Mochizuki et al., 2004). These values are consistent with the expected values of $36.2 \mu\text{T}$ for Hawaii Island (DGRF1965) and $45.5 \mu\text{T}$ for Oshima Island (DGRF 1985), suggesting that the LTD-DHT Shaw method is valid for samples with a wide range of high-temperature oxidation states. Thus, it appears possible that the use of the LTD-DHT Shaw method may give more reliable palaeointensity determinations. In this study, the validity of the LTD-DHT Shaw method is further examined by application to another historical lava with high-temperature oxidation states.

The Thellier method may prove to be more useful if pre-selection criteria can be applied to samples. The erroneously high Thellier palaeointensities of the Kilauea 1960 lava (Yamamoto et al., 2003) and Oshima 1986 lava (Mochizuki et al., 2004) were mostly obtained for samples containing titanomagnetite grains and well-developed ilmenite lamellae, corresponding to oxidation indices of III (or II) to V, as defined by Wilson and Watkins (1967) and Watkins and Haggerty (1967). Volcanic rock samples containing magnetic grains with intermediate oxidation indices may therefore be inappropriate for use with the Thellier method. The potential of such a relationship for use as a pre-selection criterion for application of the Thellier method is also investigated in this study.

The lava examined in this study is the Kilauea 1970 lava, which is regarded as a typical hot-spot basalt. The LTD-DHT Shaw method is applied to several block samples from a massive section of the lava and compared with the results of Coe's version of the Thellier method applied to the same samples.

2. Samples and magnetic properties

2.1. Samples

Samples were taken from a basaltic lava extruded in 1970 on the southeast flank of the Kilauea volcano, Hawaii Island (Fig. 1). The sampling site is located at (19.303°N, 155.174°W), where the Chain of Craters Road traverses the 1970 lava exposing a 3 m-high outcrop of a massive section of the lava flow. Five block samples (labelled A–E) were collected at a height of about 1 m from the road surface within a distance of about 10 m along the road. As a sun compass could not be used, sample orientation was determined using a magnetic compass after checking for the absence of significant deflection of magnetic north. A few cores of 25 mm diameter were drilled from the block samples and cut into one or two specimens of about 25 mm in length in the laboratory for palaeomagnetic measurements.

The DGRF 1970 field at the sampling site was calculated to be $D = 11.0^\circ$, $I = 36.8^\circ$ and $F = 35.8 \mu\text{T}$. After alternating field (AF) demagnetisation of the NRM, principal component analysis (Kirschvink, 1980) was performed to extract the primary components. The average direction for the five block samples is $D = 16.8^\circ$, $I = 38.4^\circ$ and $\alpha_{95} = 6.4^\circ$ ($N = 5$), and thus is not significantly deflected from the expected field.

2.2. Thermomagnetic analyses, hysteresis properties and LTD ratios

Thermomagnetic analyses of the Curie temperature (T_c) were performed under helium gas flow using a vibrating sample magnetometer (VSM; Micro Mag 3900, Princeton Measurements Corporation). Most of the thermomagnetic curves exhibited a major phase with $T_c > 520^\circ\text{C}$ (Fig. 2), indicating the presence of titanium-poor titanomagnetites. Minor phases with $T_c \cong 300^\circ\text{C}$ were identified in the heating curve for sample D and in the heating and cooling curves for sample E. The heating and cooling curves for samples A, B, C, and E displayed largely reversible features, although the cooling curves were somewhat lower than the heating curves possibly due to some thermal alteration during heating and/or instrumental lag in the measured temperatures between heating and cooling stages. In contrast, the difference between the heating and cooling curves for sample D is relatively large, probably due to thermal alteration during heating. Sample D also produced an unsuccessful result in the Thellier experiment (see Section 3.2).

VSM hysteresis property measurements (M_s : saturation magnetisation, M_{rs} : remanent saturation magnetisation, B_{rc} : remanent coercivity, and B_c : coercivity) were performed at room temperature using several small chips from each block sample.

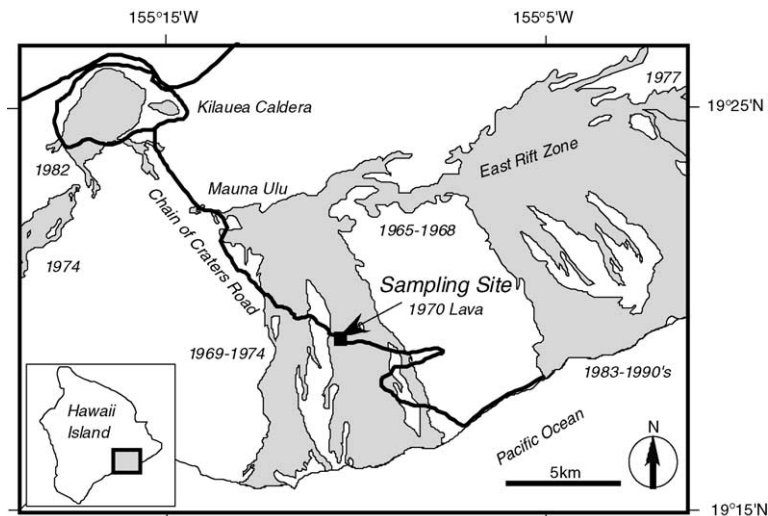


Fig. 1. Locality map of the sampling site. Samples were collected from the Kilauea 1970 lava. Shaded areas indicate the distribution of historical lavas extruded since 1965.

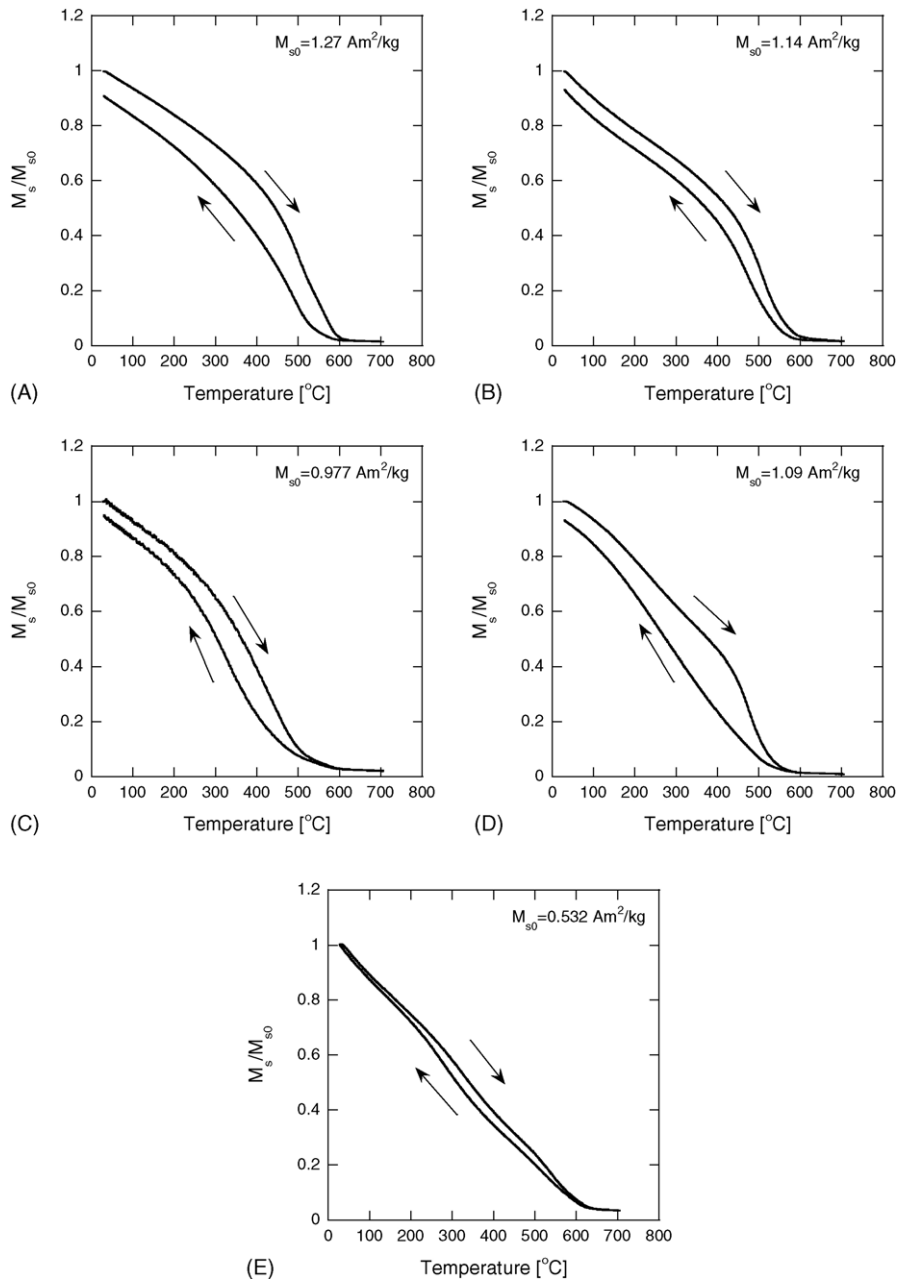
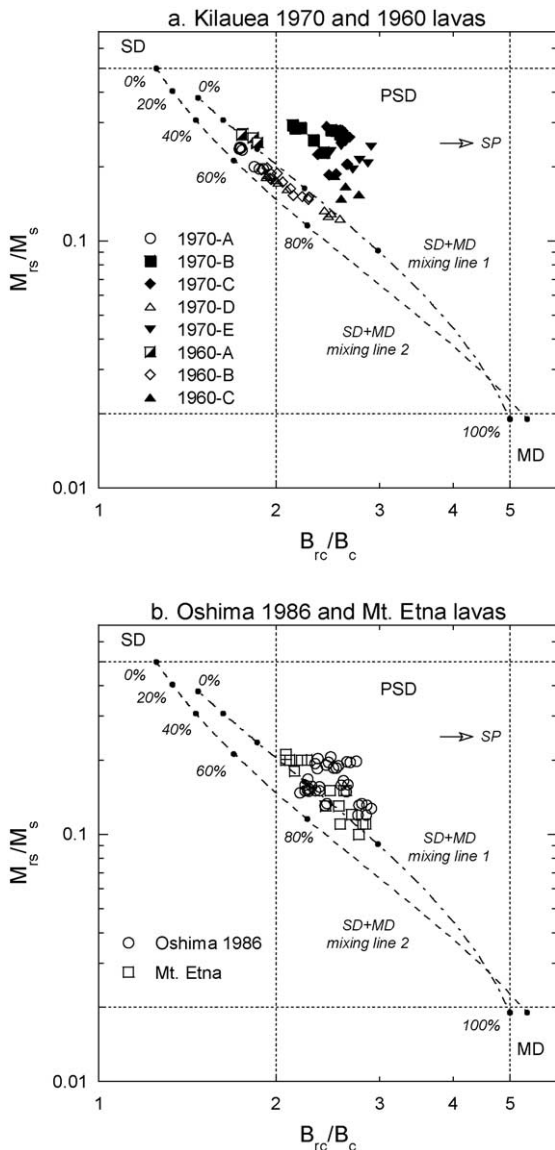


Fig. 2. Thermomagnetic curves of the block samples used in this study. The vertical axis is saturation magnetisation (M_S) normalised to that at room temperature (M_{S0}). Arrows indicate heating or cooling curves.

As shown in Fig. 3(a), the samples exhibit properties of $0.12 < M_{rs}/M_s < 0.29$ and $1.7 < B_{rc}/B_c < 2.9$, corresponding to single-domain (SD) or pseudo-single-domain (PSD) regions of the Day plot (Day et al., 1977; Dunlop, 2002a). It should be noted that the data points for samples A and D appear to be distributed along mixing lines between SD and MD components (after Dunlop, 2002a). This will be discussed in Section 4.1.



2.3. High-temperature oxidation states

Magnetic minerals exhibiting various degrees of high-temperature oxidation were observed under a reflected-light microscope with a magnification of 100–500, and the samples were free of other forms of oxidation such as low-temperature oxidation. Using oxidation indices of I–VI (Wilson and Watkins, 1967; Watkins and Haggerty, 1967), the high-temperature oxidation states were classified into three levels in the same way as Mochizuki et al. (2004): (1) a low oxidation state with oxidation indices of I–II, (2) an intermediate oxidation state with III–V, and (3) a high oxidation state with oxidation index VI (Fig. 4). All samples contained titanomagnetite grains in both low and high oxidation states. However, grains of intermediate oxidation level were not found in samples B, C and E, whereas some amount was found in samples A and D. Based on these observations, the block samples can be divided into two groups: (1) intermediate oxidation group (samples A and D) and (2) non-intermediate oxidation group (samples B, C and E). These samples were therefore deemed to be suitable for testing the reliability of palaeointensity determinations using high-temperature oxidation states.

All samples were observed to contain many vesicles of 10^2 to 10^3 μm in size under the microscope, and the high-temperature oxidation was seen to be more intensive in magnetic grains in contact with vesicles, similar to observations made for the Oshima 1986 lava (Mochizuki et al., 2004). As a more detailed investigation, the high-temperature oxidation states of magnetic

Fig. 3. (a) Day plot (Day et al., 1977; Dunlop, 2002a) of the block samples used in this study. Several small chips were taken from each block sample and measured at room temperature with a VSM. Open and closed symbols denote intermediate and non-intermediate oxidation samples, respectively. Data points of the samples from the Kilauea 1960 lava (Yamamoto et al., 2003) are also shown. Samples from 1960-A, -B and -C are of low, intermediate and high high-temperature oxidation levels, respectively (see the text). After Dunlop (2002a), the theoretical mixing lines between SD and MD end members are also shown together with ratios of MD components: mixing line 1 (dot-dashed line) assuming the end members of Day et al. (1977) and mixing line 2 (dashed line) assuming the end members of Parry (1965). The shift of mixtures with SP particles is represented by an arrow. (b) Day plot of the samples from the Oshima 1986 lava (Mochizuki et al., 2004) and the Mt. Etna lavas (Calvo et al., 2002). Other symbols are the same as above.

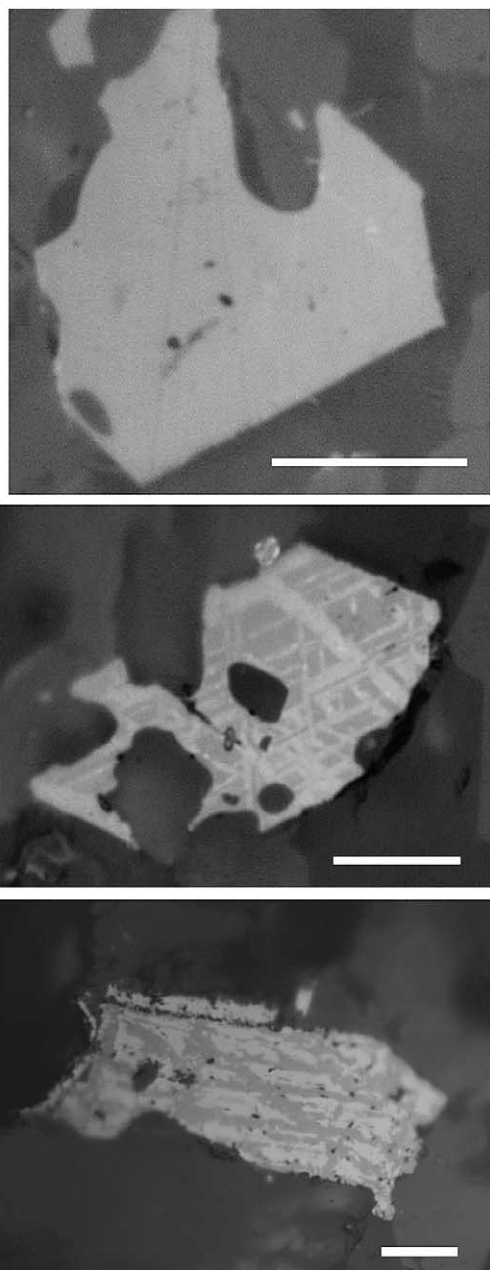


Fig. 4. Representative photographs of titanomagnetite grains taken through the reflected-light microscope: low oxidation level (sample D, top), intermediate oxidation level (sample D, middle), and high oxidation level (sample A, bottom). Bars indicate 10 μm length.

Table 1

Relative distribution of magnetic grains with respect to oxidation indices

Block sample ID observed part	Oxidation index		
	I–II	III–V	VI
Intermediate oxidation group			
A			
Surrounding vesicles	0.42	0.16	0.42
Away from vesicles	0.92	0.05	0.03
D			
Surrounding vesicles	0.26	0.10	0.64
Away from vesicles	0.96	0.02	0.02
Non-intermediate oxidation group			
B			
Surrounding vesicles	0.03	0.00	0.97
Away from vesicles	0.21	0.00	0.79
C			
Surrounding vesicles	0.19	0.00	0.81
Away from vesicles	0.87	0.00	0.13
E			
Surrounding vesicles	0.00	0.00	1.00
Away from vesicles	1.00	0.00	0.00

Several tens of grains were counted in individual regions. The samples are classified into intermediate and non-intermediate groups. Details are in the text.

grains were identified and counted in individual areas surrounding vesicles and distant from vesicle surfaces. Microscopic identification was confirmed from chemical composition measurements of some grains in each block sample by energy-dispersive x-ray spectroscopy (EDS). The results are summarised in Table 1.

In the intermediate oxidation group (samples A and D), 10–16% of titanomagnetite grains surrounding vesicles were in an intermediate oxidation state, while 42–64% were in a high oxidation state (Table 1). Further from vesicle surfaces, only 2–5% of grains were in an intermediate oxidation state, while most (92–96%) were in a low oxidation state. Therefore, the areas away from vesicles have been subjected to a relatively low degree of high-temperature oxidation. In the non-intermediate oxidation group (samples B, C and E), more than 80% of grains surrounding vesicles were in the high oxidation state, and no grains of intermediate oxidation state were found. In areas away from the vesicle surfaces, the fraction of grains in the high oxidation state varied from 0 to 79%.

Table 2
Palaeointensity results of the LTD-DHT Shaw method

Specimen ID	NRM ₀ [*] (10 ⁻⁵ A m ² /kg)	LTD ratio	1st heating						2nd heating				F _L (μT)	F ± σ _F (μT)
			H _L	Slope _{A1}	Slope _N	f _N	r _N	H _L	Slope _{A2}	Slope _T	f _T	r _T		
A-02-1	341	0.174	0	0.919	1.22 ± 0.01	1.000	0.999	0	1.02	<i>0.926</i>	1.000	1.000	30.0	–
A-02-2	346	0.170	5	0.940	1.20 ± 0.01	0.934	0.999	0	0.969	1.01	1.000	0.999	30.0	36.0 ± 0.4
A-11-2	254	0.304	30	0.909	1.15 ± 0.02	0.304	0.995	0	0.969	1.01	1.000	1.000	30.0	34.6 ± 0.7
B-01-2	604	0.132	15	0.823	1.51 ± 0.01	0.890	1.000	5	0.980	0.982	1.000	1.000	30.0	45.3 ± 0.2
B-02-1	711	0.099	5	0.976	1.21 ± 0.01	0.969	1.000	0	1.01	0.979	1.000	1.000	30.0	36.3 ± 0.1
B-03-1	501	0.096	15	1.00	1.24 ± 0.01	0.932	1.000	0	0.982	1.03	1.000	1.000	30.0	37.3 ± 0.1
C-02-2	286	0.123	10	0.970	1.24 ± 0.01	0.811	0.999	0	0.956	1.03	1.000	1.000	30.0	37.3 ± 0.3
C-11-1	426	0.103	10	0.978	1.29 ± 0.01	0.878	1.000	0	0.986	0.975	1.000	1.000	30.0	38.8 ± 0.1
C-12-3	273	0.131	10	1.02	1.26 ± 0.01	0.777	0.999	0	1.01	0.956	1.000	0.999	30.0	37.8 ± 0.3
D-02-1	225	0.131	10	0.950	1.27 ± 0.01	0.729	1.000	0	0.990	0.980	1.000	0.999	30.0	38.1 ± 0.2
D-04-1	232	0.141	0	0.955	1.32 ± 0.01	1.000	0.999	0	0.968	0.992	1.000	1.000	30.0	39.6 ± 0.3
E-01-2	272	0.114	0	0.977	1.26 ± 0.01	1.000	1.000	0	1.00	0.987	1.000	1.000	30.0	37.9 ± 0.2
Average														38.2 ± 2.8 (N = 11), 37.4 ± 1.4 (N = 10)

NRM₀: NRM intensity before LTD; LTD ratio: a ratio of the LTD-erased component to the initial NRM; H_L: the lowest AF step of the linear portion; slope_{A1} and slope_{A2}: slopes of the portion with AF steps > H_L in the ARM0–ARM1 and ARM1–ARM2 diagrams, respectively; slope_N and slope_T: a slope of the linear portion in the NRM–TRM1^{*} and TRM1–TRM2^{*} diagrams, respectively; f_N: NRM fraction of the linear portion in the NRM–TRM1^{*} diagram; f_T: TRM fraction of the linear portion in the TRM1–TRM2^{*} diagram; r_N and r_T: correlation coefficients of the linear portions in the NRM–TRM1^{*} and TRM1–TRM2^{*} diagrams, respectively; F_L: laboratory field; F and σ_F: palaeointensity and its error. The averaged palaeointensity is calculated from all the results passing the selection criteria (N = 11) and also from the results except for B-01-2 (N = 10). The italic value does not fulfill the selection criteria (sample A-02-1).

These observations imply that in addition to the cooling rate, the high-temperature oxidation of the present samples was strongly controlled by the oxygen fugacity of the fluid phase in vesicles and by the oxygen permeability of the regions around vesicles. It is likely that the high-temperature oxidation of the samples progressed during the initial cooling stage and thus more intensively in the immediate area around vesicles.

3. Palaeointensity measurements and results

3.1. LTD-DHT Shaw method

The LTD-DHT Shaw method (Tsunakawa et al., 1997; Yamamoto et al., 2003) was applied to these samples using the ARM correction technique of Rolph and Shaw (1985) for correction of the TRM for thermal alteration of the samples during laboratory heating. Samples were heated twice in a vacuum of 10 to 10^2 Pa at 610 °C. The peak temperature was held for 20 and 30 min in the first and second heating stage, respectively. The TRM was induced by application of a 30 μ T dc field during the heating and cooling stages, and the ARM was induced by the application of a 100 μ T dc field. Samples were subjected to step-wise AF demagnetisation in 5–10 mT intervals up to 160 mT. All remanences were measured using an automated spinner magnetometer with AF demagnetiser (Natsuhara-Giken Dspin-2; Kono et al., 1984, 1997). The details of the experimental procedures are as described in Yamamoto et al. (2002, 2003) and Mochizuki et al. (2004).

The selection criteria adopted in the application of the LTD-DHT Shaw method (Yamamoto et al., 2003; Mochizuki et al., 2004) in this study are given below, where the magnetisations after the first and the second heating steps are denoted by suffixes of 1 and 2, and TRM after ARM correction is denoted by TRM*.

- (1) The stable primary component must be recognisable in orthogonal plots of the AF demagnetisation of NRM.
- (2) The slope of the relation in the TRM1–TRM2* diagram (slope_T) must be unity within experimental error, typically $1.05 \geq \text{slope}_T \geq 0.95$ in this study.
- (3) The linear portions of the relation in the NRM–TRM1* diagram must not be less than 15% of the original NRM ($f_N \geq 0.15$). The same con-

dition must be satisfied for the TRM1–TRM2* diagram ($f_T \geq 0.15$). The associated correlation coefficients should also be no less than 0.995 ($r_N, r_T \geq 0.995$). Slopes of the corresponding coercivity portion in the ARM0–ARM1 and ARM1–ARM2 diagrams are defined by slope_{A1} and slope_{A2} , respectively.

The results are summarised in Table 2, and representative NRM–TRM1* diagrams are shown in Fig. 5. Eleven out of the 12 specimens passed the selection criteria. The failed specimen was from sample A, with failure in the double heating test ($\text{slope}_T = 0.926$). The resultant palaeointensities range from 34.6 to 45.3 μ T with an average of $38.2 \pm 2.8 \mu$ T ($N = 11, \pm 1\sigma$), consistent with the expected value of 35.8 μ T (DGRF 1970).

Specimen B-01-2 yielded a palaeointensity (45.3 μ T) that was 27% higher than the expected value. As this result affords the smallest slope_{A1} (0.823) of the present measurements (Table 2), this high palaeointensity may have been induced by a significant change in the ARM coercivity spectra during the first heating step. However, as similar changes in ARM coercivity have usually given reasonable values in previous studies (Tsunakawa and Shaw, 1994; Yamamoto et al., 2003; Mochizuki et al., 2004), this interpretation is not conclusive. If the palaeointensity of B-01-2 is excluded as an outlier, the average is calculated to be $37.4 \pm 1.4 \mu$ T ($N = 10$).

Most of the specimens yielded large linear fractions ($f_N > 0.7$). However, specimen A-11-2 displayed a relatively small fraction of NRM ($f_N = 0.304$), attributable to the inclusion of a secondary component with coercivity of less than 30 mT, possibly of isothermal or viscous origin.

3.2. Thellier method

Coe's version of the Thellier method (Coe, 1967) was also applied to nine specimens from the same block samples examined in the LTD-DHT Shaw experiments. Specimens were heated at 100–600 °C in 20–50 °C steps in air. The reproducibility of the peak temperature in each heating step was better than 1 °C. The hold time at the peak temperature was set at 15 min. The laboratory dc field intensity was maintained at 30 μ T throughout the heating and cooling cycles for TRM

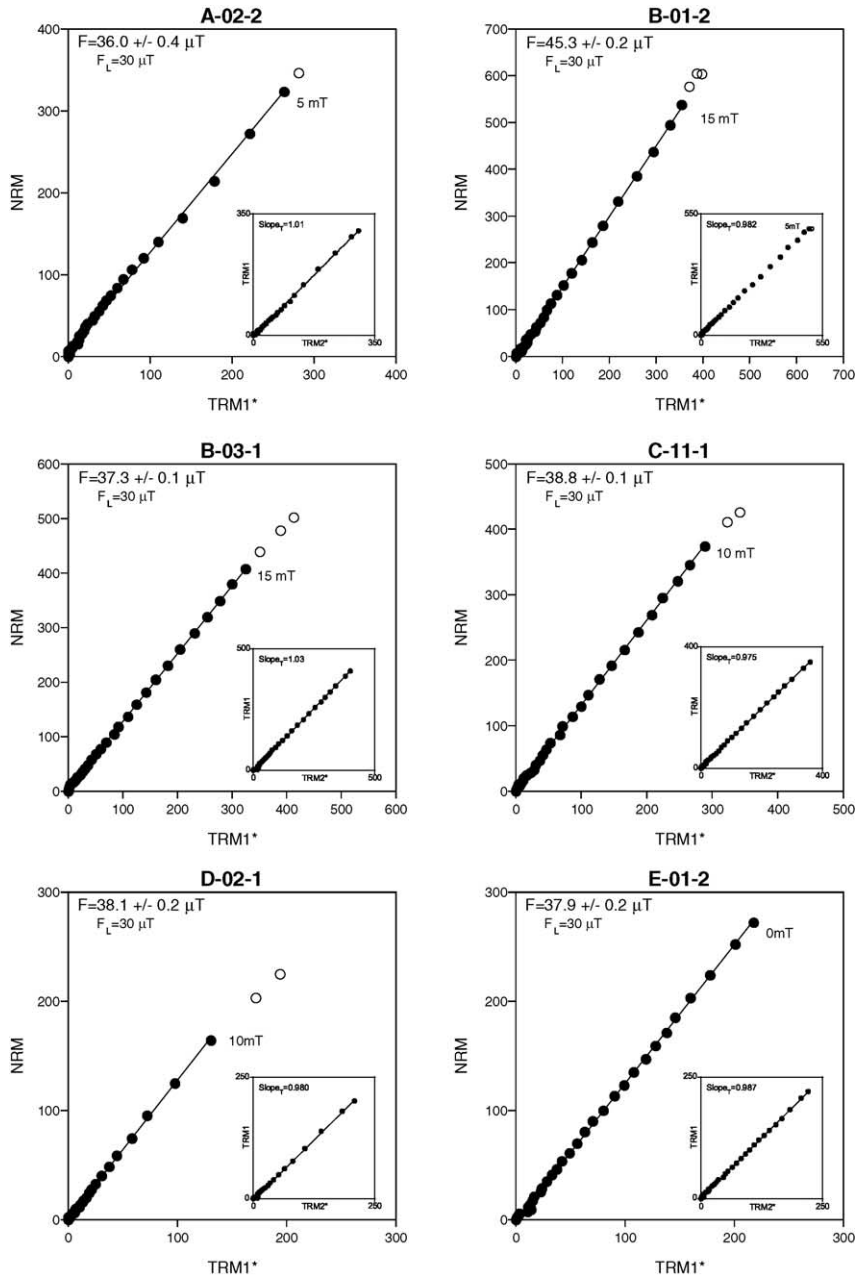


Fig. 5. Representative diagrams of NRM vs. TRM1* by the LTD-DHT Shaw method. Units are $10^{-5} \text{ A m}^2/\text{kg}$. Closed circles indicate the linear portion used in the palaeointensity calculation. The lowest coercivity of the linear portion is attached to the least-square-fit line. It is noted that all the remanences are treated with LTD and the applicability of the ARM correction (Rolph and Shaw, 1985) was examined by the double heating test as in TRM1–TRM2* diagrams. The results are summarised in Table 2 and details are in Section 3.1.

development. In the pTRM checks, the agreement between the TRM values of the present and one or two previous temperature steps was tested. Magnetic susceptibility was measured at room temperature using a susceptibility meter (MS2, Bartington Instruments) after each heating step. The details of the procedures are as described in Yamamoto et al. (2003) and Mochizuki et al. (2004).

Although stringent selection criteria for Thellier-type results have been proposed (e.g. Selkin and Tauxe, 2000), there appear to be no definite selection criteria for the Thellier method (e.g. Calvo et al., 2002; Biggin and Thomas, 2003). In this study, the selection criteria of Mochizuki et al. (2004) are tentatively employed, as given below:

- (1) The stable primary component must be recognisable in the orthogonal plot of the thermal demagnetisation of NRM (zero-field NRM).
- (2) The linear portion of the primary component in the Arai diagram must be defined by four or more points ($N \geq 4$) and must correspond to no less than 15% of the original NRM ($f \geq 0.15$).
- (3) The linear portion must have positive pTRM checks. The pTRM check is judged from agreement between the reproduced pTRM and the TRM at the 2σ level. This error (σ_{pTRM}) is calculated from experimental uncertainties of remanence measurements (σ_{meas}), heating temperature (σ_{temp}) and applied dc fields (σ_{DC}), that is, $\sigma_{\text{pTRM}}^2 = \sigma_{\text{meas}}^2 + \sigma_{\text{temp}}^2 + \sigma_{\text{DC}}^2$.
- (4) The quality factor (Coe et al., 1978) must not be lower than 5 ($q \geq 5$).

Representative results are shown in Fig. 6. Seven out of the nine specimens passed these selection criteria. The two failed specimens were rejected because of low q values (Table 3). For the seven palaeointensities obtained for block samples A, B, C and E by the Thellier method, the linear portions with positive pTRM checks extend to relatively high temperatures of 500–600 °C ($f \geq 0.43$). The resultant palaeointensities range from 35.5 to 55.4 μT , with $q = 7.1$ –64.0. Susceptibility changes were less than 10% of the initial values for the linear portions.

These seven results give an average of $43.2 \pm 8.4 \mu\text{T}$ ($N = 7$), approximately 21% higher than the expected value of 35.8 μT . However, the standard deviation is so large that the average is statistically consistent with the

expected value at the 1σ level. This large standard deviation is obviously caused by two anomalously high values (52.1 and 55.4 μT) from sample A (intermediate oxidation group). If these two values are excluded as outliers, the average for samples B, C and E give a reasonable result with a smaller standard deviation ($37.9 \pm 1.7 \mu\text{T}$, $N = 5$). This suggests that the high Thellier palaeointensities obtained for sample A may not be due to strong local magnetic anomalies but to the specific magnetic property of the rock itself.

The two specimens that failed, A-11-1 and D-01-1, were rejected due to the low q values of the linear portion associated with positive pTRM checks (Table 3). The NRM–TRM diagrams display upward concave features (Fig. 6), yielding relatively small linear portions ($f = 0.304$ and 0.259). The calculated palaeointensities were 46.8 and 45.2 μT for A-11-1 and D-01-1, respectively. These values are not used in the later discussion.

Orthogonal plots of NRMs remaining after zero-field heating (thermal demagnetisation of NRM) are shown in the core-coordinate system in Fig. 6, where the z axis is parallel to the core axis and anti-parallel to the applied dc field. The NRM direction of sample D-01-1 gradually approaches the $-z$ direction, suggestive of thermal alteration associated with chemical remanent magnetisation (CRM) acquisition parallel to the applied laboratory field. This directional change makes it difficult to recognise the primary NRM component of D-01-1, which is another reason why this sample was discarded in the Thellier experiments. The failure of D-01-1 can probably be attributed to thermal alteration in the laboratory. Such thermal alteration due to laboratory heating is not always detected by pTRM checks (e.g. Riisager and Riisager, 2001; Valet, 2003; Mochizuki et al., 2004). The thermal alteration can also be estimated based on the intensity ratio of laboratory CRM to NRM after zero-field heating at a certain temperature. This value, denoted γ (Mochizuki et al., 2004), can be used to determine whether samples may have undergone thermal alteration. The parameter γ is defined as

$$\gamma = \sin \theta / [\sin \theta + \sin(\varphi - \theta)],$$

where θ is the angle between the directions of initial NRM and NRM after zero-field heating, and φ the angle between the initial NRM and laboratory CRM directions (Mochizuki et al., 2004). In this study, θ and

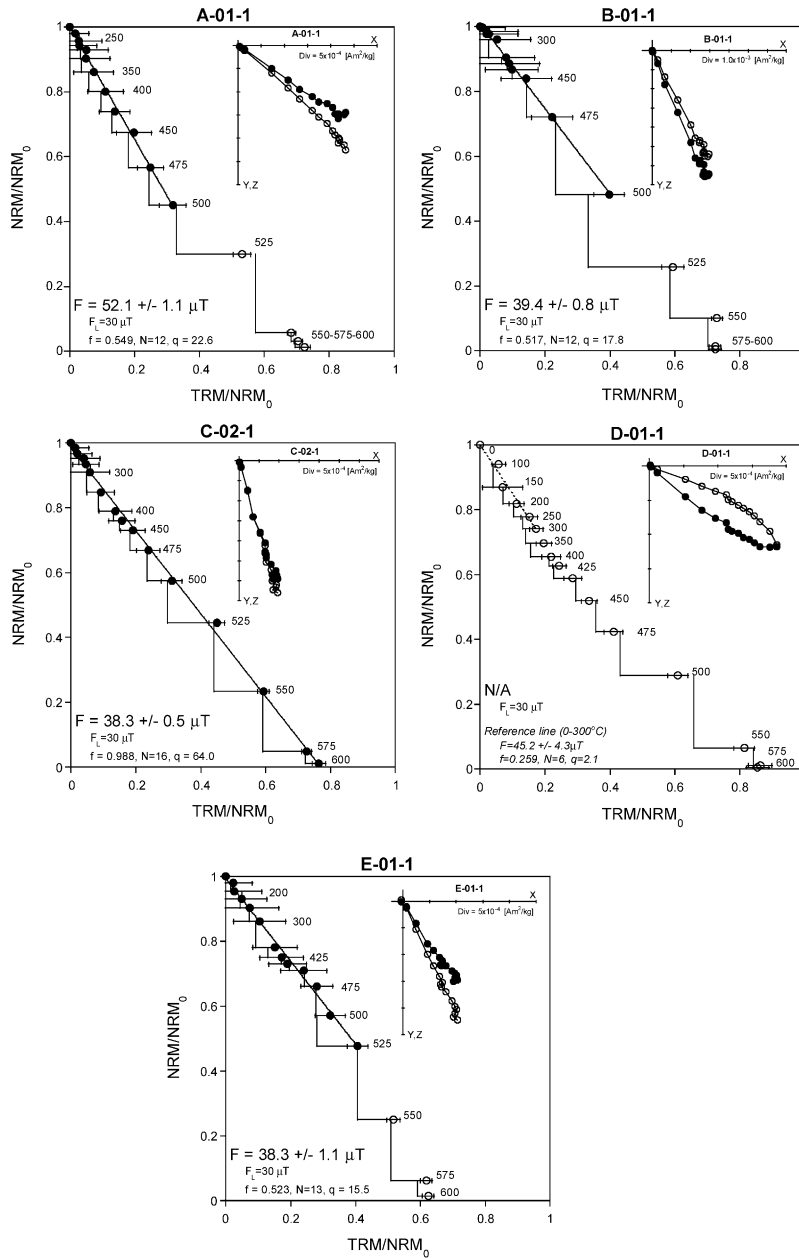


Fig. 6. Representative Arai diagrams of Coe's version of the Thellier method. Closed circles describe the linear portion used in the palaeointensity calculation and the least-square-fit line is shown as solid. Error bars are at the 2σ level. Sample D-01-1 did not pass the selection criteria and its reference line is shown as dotted. The orthogonal plots of NRM after zero-field heating are shown in the core-coordinate system: closed circles on the X–Y plane and open circles on the X–Z plane. The results are summarised in Table 3 and details are in Section 3.2.

Table 3
Palaeointensity results of the Thellier method

Specimen ID	NRM ₀ (10 ⁻⁵ A m ² /kg)	ΔT (°C)	N	r	f	g	q	Slope	F _L (μT)	F ± σ _F (μT)	γ _{lin}	γ _{all}
A-01-1	355	0–500	12	0.998	0.549	0.866	22.6	1.74 ± 0.04	30.0	52.1 ± 1.1*	0.09	0.14
A-01-2	304	0–500	10	0.991	0.529	0.881	9.7	1.85 ± 0.09	30.0	55.4 ± 2.7*	0.12	0.14
A-11-1	322	0–440	7	0.968	0.304	0.824	2.2	1.56 ± 0.18	30.0	(46.8 ± 5.4)	–	0.13
B-01-1	903	0–500	12	0.998	0.517	0.716	17.8	1.31 ± 0.03	30.0	39.4 ± 0.8	0.03	0.13
B-02-2	453	0–500	10	0.988	0.463	0.865	7.1	1.36 ± 0.08	30.0	40.8 ± 2.3	0.12	0.15
C-02-1	452	0–600	16	0.999	0.988	0.877	64.0	1.28 ± 0.02	30.0	38.3 ± 0.5	0.09	0.09
C-12-2	274	0–600	15	0.997	0.989	0.910	45.3	1.18 ± 0.02	30.0	35.5 ± 0.7	0.07	0.07
D-01-1	248	0–300	6	0.982	0.259	0.788	2.1	1.51 ± 0.14	30.0	(45.2 ± 4.3)	–	0.18
E-01-1	286	0–525	13	0.995	0.523	0.884	15.5	1.28 ± 0.04	30.0	38.3 ± 1.1	0.09	0.12
Average										43.2 ± 8.4 (N=7), 37.9 ± 1.7 (N=5*)		

NRM₀: NRM intensity at room temperature; ΔT: temperature interval used in the palaeointensity calculation; N and r: the number of data and the associated correlation coefficient of the linear portion; f, g and q: NRM fraction, gap factor and quality factor, respectively (Coe et al., 1978); F_L: laboratory field; F and σ_F: palaeointensity and its error; γ_{lin}: maximum CRM ratio for the linear portion; γ_{all}: maximum CRM ratio for all the temperature steps except 600 °C. The italic value is in contradiction to the selection criteria and the calculated F is discarded. The averaged palaeointensity is calculated from all the results passing the selection criteria (N = 7) and also from all results except the two results (A-01-1 and A-01-2; N = 5*). The parenthesised palaeointensity is shown as a reference value because the corresponding result does not satisfy the selection criteria.

φ are calculated as follows:

$$\theta = I_S \text{ (initial NRM)}$$

$$- I_S \text{ (NRM after zero-field heating),}$$

$$\varphi = I_S \text{ (initial NRM)} - (-90^\circ),$$

where I_S is the core-coordinate inclination. The maximum values of γ for the linear portion of the relation in the Arai diagram (γ_{lin}) and for all temperature steps except 600 °C (γ_{all}) are summarised in Table 3. According to Mochizuki et al. (2004), the samples yielding erroneously high Thellier palaeointensities have larger γ_{lin} values than other samples. Block sample A, however, exhibits γ_{lin} and γ_{all} values comparable to the other samples, suggesting that the effect of thermal alteration during laboratory heating is minor in the present experiments.

3.3. Summary of palaeointensity results

The palaeointensities obtained by the LTD-DHT Shaw method are consistent with the expected values, whereas the values determined by the Thellier method for intermediate oxidation samples are anomalously high. Therefore, the LTD-DHT Shaw method appears

to be applicable irrespective of the high-temperature oxidation state, whilst the Thellier method tends to give erroneously high palaeointensities for samples with intermediate oxidation levels. It should be noted that the Thellier method was found to be valid for non-intermediate samples, as shown by Yamamoto et al. (2003) and Mochizuki et al. (2004).

4. Discussion

4.1. Possible pre-selection techniques for Thellier experiments

The hysteresis parameters of the intermediate oxidation group exhibit a characteristic trend on the Day plot, whereas the non-intermediate oxidation group produces a cluster of data points (Fig. 3(a)). These features can be seen clearly when compared with the data set for the Kilauea 1960 lava (Yamamoto et al., 2003; Fig. 3(a)). According to the classification by Yamamoto et al. (2003), the samples from group B (1960-B) contain grains with oxidation indices of II–V and thus correspond to the intermediate oxidation group, while those from group A (1960-A; oxidation index of I) and

group C (1960-C; VI) represent a non-intermediate oxidation group. Therefore, the 1960 lava samples exhibit the same characteristics as the 1970 lava on the Day plot.

Theoretical mixing lines between SD and MD are also shown in Fig. 3(a) for two representative pairs of end members (SD + MD mixing lines 1 and 2; Dunlop, 2002a). Those lines fall close to the data points of the intermediate oxidation group. If magnetic grains of the intermediate oxidation samples are assumed to be composed of SD + MD mixtures (represented by mixing line 2), the estimated MD volume fractions are 60–80%. The corresponding fractions of MD remanence are 5–13% based on the M_{rs}/M_s ratio of 0.019 for MD and 0.5 for SD (Parry, 1965; Dunlop, 2002a).

The MD content can also be estimated by applying LTD treatment of NRM at liquid nitrogen temperature in the LTD-DHT Shaw experiments (see Section 3.1). LTD treatment erases the MD component of titanium-poor titanomagnetites (e.g. Ozima et al., 1964; Heider et al., 1992), and is thus expected to be effective for the present samples, the main phase of which is considered to be titanium-poor titanomagnetite. The ratios of the LTD-erased component to the initial NRM intensity are listed as LTD ratios in Table 2. According to those ratios, the MD remanences are estimated to be 10–17% of the initial NRM, except for specimen A-11-2 (about 30%). These MD remanence fractions are not discordant with those estimated from the SD + MD mixing model (Fig. 3(a)).

An alternative interpretation of the characteristic trend seen in Fig. 3(a) is that the samples contain a number of PSD grains, as suggested by the distribution of experimental data points for PSDs around the SD + MD mixing lines (Dunlop, 2002a). It is noted that either grain assemblage is reasonable for titanomagnetites of intermediate oxidation levels, which are subdivided by numerous ilmenite lamellae.

The cluster of data for the non-intermediate oxidation group shifts from the SD + MD (or PSD/SD + MD) mixing lines towards regions of mixtures with superparamagnetic (SP) grains, as shown by Dunlop (2002a, 2002b). Therefore, the samples distant from the mixing line possibly contain significant amounts of SP grains, suggesting that severe thermal alteration during natural cooling may produce SP-sized domains in titanomagnetites and/or new SP particles in paramagnetic minerals.

For volcanic rocks other than hot-spot basalts, hysteresis properties of the Oshima 1986 lava (Mochizuki et al., 2004) and the Mt. Etna lavas (Calvo et al., 2002) are plotted in Fig. 3(b). They are distributed generally between the theoretical mixing lines and the cluster of the non-intermediate oxidation group of the Kilauea lavas. According to Mochizuki et al. (2004) and Calvo et al. (2002), those samples contain some amount of intermediate oxidation grains and their Thellier palaeointensities often resulted in overestimation by about 30%. It is inferred from Fig. 3(a) and (b) that the distance of samples from the SD + MD (or PSD/SD + MD) mixing lines on the Day plot can be utilised as an index of the sample pre-selection in the Thellier experiment.

4.2. Reasons for the broad applicability of the LTD-DHT Shaw method

The broad applicability of the LTD-DHT Shaw method for samples with high-temperature oxidation and the possible causes of the erroneously high Thellier palaeointensities have been discussed in previous studies. Yamamoto et al. (2003) suggested that the high Thellier palaeointensities obtained for intermediate oxidation samples from the Kilauea 1960 lava were caused by thermochemical remanent magnetisation (TCRM) during natural cooling. They also indicated that TCRM-affected samples could be efficiently rejected based on the non-linearity of the relation in the NRM–TRM1* diagram or non-unity of the TRM1–TRM2* relation. Mochizuki et al. (2004) implied that the high Thellier palaeointensities obtained for the Oshima 1986 lava could be attributed to the effect of thermal alteration during laboratory heating at low temperatures. According to their interpretation, an intermediate degree of high-temperature oxidation could mean that oxidation may have stopped during natural cooling and then restarted during laboratory heating. Whereas the effects of thermal alteration on laboratory-induced TRMs can be corrected through the application of the ARM correction technique in the LTD-DHT Shaw method, the effects on NRM and pTRMs are sometimes undetectable by the usual Thellier method (Mochizuki et al., 2004).

If the high Thellier values are attributed to MD components (e.g. Levi, 1977; Xu and Dunlop, 1995), LTD treatment and AF demagnetisation may in fact coun-

teract possible MD effects on NRM, TRM and ARM in the LTD-DHT Shaw experiment. In the case of PSD effects (e.g. Kosterov and Prévot, 1998), the coercivity spectra of ARM and TRM may reflect the physical change of PSD grains during laboratory heating, thus rendering the PSD effect detectable or correctable in the LTD-DHT Shaw method.

Magnetic interaction between different phases (e.g. Mankinen and Champion, 1993) or different domains (e.g. Mochizuki et al., 2004) may also be a cause of the high Thellier values. In this regard, the LTD-DHT Shaw procedure for obtaining the full TRM by heating samples above their Curie temperatures and cooling to room temperature in a constant dc field appears to be more analogous to the natural process than the step-wise heating and cooling cycles applied for pTRM acquisition in the Thellier experiment, where the pTRM direction induced by the applied laboratory field is not usually parallel to the remaining NRM direction. By this analogy, the magnetic interaction during natural cooling appears to be followed more closely by the LTD-DHT Shaw method than by the Thellier method, although the details remain unclear.

5. Conclusions

The LTD-DHT Shaw method for determining palaeointensities was applied to five block samples from a massive section of the Kilauea 1970 lava. Results were obtained for 11 of the 12 specimens prepared from those samples, yielding an average palaeointensity of $38.2 \pm 2.8 \mu\text{T}$ ($N=11$). This result is consistent with the expected value determined from DGRF 1970 ($35.8 \mu\text{T}$) at the 1σ level, demonstrating that the LTD-DHT Shaw method is valid for a wide range of high-temperature oxidation states.

Coe's version of the Thellier method was also applied to nine specimens prepared from the same block samples used in the LTD-DHT Shaw experiments. Seven of the specimens passed the selection criteria, and the palaeointensities of the passed specimens varied widely, from 35.5 to $55.4 \mu\text{T}$. The average was $43.2 \pm 8.4 \mu\text{T}$ ($N=7$), which due to the large standard deviation is also consistent with the expected value at the 1σ level. Passed specimens from one block sample yielded anomalously high palaeointensities of 52.1 and $55.4 \mu\text{T}$, and on further inspection

were found to contain titanomagnetites of intermediate high-temperature oxidation level with oxidation indices of III–V. Excluding the palaeointensities of those specimens, the average by the Thellier method became closer to the expected value with a smaller standard deviation ($37.9 \pm 1.7 \mu\text{T}$, $N=5$). Therefore, the Thellier method is valid at least for non-intermediate oxidation samples from the Kilauea 1970 lava.

Finally, samples lying close to the SD+MD (or PSD/SD+MD) mixing lines on the Day plot were found to give erroneously high Thellier palaeointensities. This relationship may therefore be a potential pre-selection criterion for application of the Thellier method.

Acknowledgements

The authors thank Yozo Hamano (University of Tokyo) and Arata Yoshihara (Toyama University) for assistance with rock magnetic measurements. Gratitude is also extended to John Shaw and anonymous referee for valuable comments.

References

- Biggin, A., Thomas, D.N., 2003. The application of acceptance criteria to results of Thellier palaeointensity experiments performed on samples with pseudo-single-domain-like characteristics. *Phys. Earth Planet. Inter.* 138, 279–287.
- Calvo, M., Prévot, M., Perrin, M., Riisager, J., 2002. Investigating the reasons for the failure of palaeointensity experiments: a study on historical lava flows from Mt. Etna (Italy). *Geophys. J. Int.* 149, 44–63.
- Coe, R.S., 1967. The determination of paleointensities of the Earth's magnetic field with emphasis on mechanisms which could cause non-ideal behavior in Thellier's method. *J. Geomagn. Geoelectr.* 19, 157–179.
- Coe, R.S., Grommé, S., Mankinen, E.A., 1978. Geomagnetic paleointensities from radiocarbon-dated lava flows on Hawaii and the question of the Pacific nondipole low. *J. Geophys. Res.* B 83, 1740–1756.
- Day, R., Fuller, M., Schmidt, V.A., 1977. Hysteresis properties of titanomagnetites: grain-size and compositional dependence. *Phys. Earth Planet. Inter.* 13, 260–267.
- Dunlop, D.J., 2002a. Theory and application of the Day plot (Mrs/Ms versus Hcr/Hc). 1. Theoretical curves and tests using titanomagnetite data. *J. Geophys. Res.* B 107, doi:10.1029/2001JB000486.
- Dunlop, D.J., 2002b. Theory and application of the Day plot (Mrs/Ms versus Hcr/Hc). 2. Application to data for rocks, sediments, and soils. *J. Geophys. Res.* B 107, doi:10.1029/2001JB000487.

- Heider, F., Dunlop, D.J., Soffel, H.C., 1992. Low-temperature and alternating field demagnetization of saturation remanence and thermoremanence in magnetite grains (0.037 μm to 5 mm). *J. Geophys. Res.* B 97, 9371–9381.
- Kirschvink, J.L., 1980. The least-squares line and plane and the analysis of paleomagnetic data. *Geophys. J. Roy. Astron. Soc.* 62, 699–718.
- Kono, M., 1978. Reliability of palaeointensity methods using alternating field demagnetization and anhysteretic remanences. *Geophys. J. Roy. Astron. Soc.* 54, 241–261.
- Kono, M., Hamano, Y., Nishitani, T., Toshi, T., 1984. A new spinner magnetometer: principles and techniques. *Geophys. J. Roy. Astron. Soc.* 67, 217–227.
- Kono, M., Kitagawa, H., Tanaka, H., 1997. Use of automatic spinner magnetometer–AF demagnetizer system for magnetostratigraphy and paleosecular variation studies. In: Eighth Scientific Assembly IAGA, Uppsala.
- Kosterov, A.A., Prévot, M., 1998. Possible mechanisms causing failure of Thellier palaeointensity experiments in some basalts. *Geophys. J. Int.* 134, 554–572.
- Levi, S., 1977. The effect of magnetite particle size on paleointensity determinations of the geomagnetic field. *Phys. Earth Planet. Inter.* 13, 245–259.
- Mankinen, E.A., Champion, D.E., 1993. Broad trends in geomagnetic paleointensity on Hawaii during Holocene time. *J. Geophys. Res.* B 98, 7959–7976.
- Mochizuki, N., Tsunakawa, H., Oishi, Y., Wakai, S., Wakabayashi, K., Yamamoto, Y., 2004. Palaeointensity study of the Oshima 1986 lava in Japan: implications for the reliability of the Thellier and LTD-DHT Shaw methods. *Phys. Earth Planet. Inter.* 146, 395–416.
- Ozima, M., Ozima, M., Akimoto, S., 1964. Low temperature characteristics of remanent magnetization of magnetite—self-reversal and recovery phenomena of remanent magnetization. *J. Geomagn. Geoelectr.* 16, 165–177.
- Parry, L.G., 1965. Magnetic properties of dispersed magnetic powders. *Phil. Mag.* 11, 303–312.
- Riisager, P., Riisager, J., 2001. Detecting multidomain magnetic grains in Thellier palaeointensity experiments. *Phys. Earth Planet. Inter.* 125, 111–117.
- Rolph, T.C., Shaw, J., 1985. A new method of paleofield magnitude correction for thermally altered samples and its application to Lower Carboniferous lavas. *Geophys. J. Roy. Astron. Soc.* 80, 773–781.
- Selkin, P.A., Tauxe, L., 2000. Long-term variations in palaeointensity. *Phil. Trans. Roy. Soc. London, Ser. A* 358, 1065–1088.
- Shaw, J., 1974. A new method of determining the magnitude of the palaeomagnetic field: application to five historic lavas and five archaeological samples. *Geophys. J. Roy. Astron. Soc.* 39, 133–141.
- Tanaka, H., Kono, M., 1991. Preliminary results and reliability of palaeointensity studies on historical and ^{14}C dated Hawaiian lavas. *J. Geomagn. Geoelectr.* 43, 375–388.
- Thellier, E., Thellier, O., 1959. Sur l'intensité du champ magnétique terrestre dans le passé historique et géologique. *Ann. Geophys.* 15, 285–376.
- Tsunakawa, H., Shaw, J., 1994. The Shaw method of palaeointensity determinations and its application to recent volcanic rocks. *Geophys. J. Int.* 118, 781–787.
- Tsunakawa, H., Shimura, K., Yamamoto, Y., 1997. Application of double heating technique of the Shaw method to the Brunhes epoch volcanic rocks. In: Eighth Scientific Assembly IAGA, Uppsala.
- Valet, J.-P., 2003. Time variations in geomagnetic intensity. *Rev. Geophys.* 41, 1004, doi:10.1029/2001RG000104.
- Watkins, N.D., Haggerty, S.E., 1967. Primary oxidation variation and petrogenesis in a single lava. *Contr. Miner. Petrol.* 15, 251–271.
- Wilson, R.L., Watkins, N.D., 1967. Correlation of petrology and natural magnetic polarity in Columbia Plateau basalts. *Geophys. J. Roy. Astron. Soc.* 12, 405–424.
- Xu, S., Dunlop, D.J., 1995. Thellier paleointensity determination using PSD and MD grains (abstr.). *Eos Trans. Am. Geophys. Union* 76 (suppl.), F170.
- Yamamoto, Y., Shimura, K., Tsunakawa, H., Kogiso, T., Uto, K., Barszczus, H.G., Oda, H., Yamazaki, T., Kikawa, E., 2002. Geomagnetic paleosecular variation for the past 5Ma in the Society Islands, French Polynesia. *Earth Planets Space* 54, 797–802.
- Yamamoto, Y., Tsunakawa, H., Shibuya, H., 2003. Palaeointensity study of the Hawaiian 1960 lava: implications for possible causes of erroneously high intensities. *Geophys. J. Int.* 153, 263–276.